Mine Water Environ (2017) 36:226–238
DOI 10.1007/s10230-016-0398-0

TECHNICAL ARTICLE

Secondary Sulphate Minerals in a Cyprus-Type Ore Deposit, Apliki, Cyprus: Mineralogy and Its Implications Regarding the Chemistry of Pit Lake Waters

Danae N. Antivachis[1] · **Elias Chatzitheodoridis**[2] · **Nikolaos Skarpelis**[1] · **Konstantinos Komnitsas**[3]

Received: 25 June 2015 / Accepted: 29 March 2016

Abstract The Apliki mine, a Cyprus-type massive sulphide deposit in Cyprus, was exploited for copper until the mid-1970s. Abandonment of the mine left a deep pit that now hosts a lake fed by surface runoff from the surrounding mineralized zone and hydrothermally altered basalt. Oxidation of the sulphide minerals and factors such as climate and terrain relief control the water–rock interactions that generate acid mine drainage (AMD), which ultimately affects and defines the quality of the lake waters. Pyrite and chalcopyrite constitute an almost inexhaustible sulphide source that leads to the formation of a variety of secondary iron and copper mineral phases. The secondary mineral assemblages in the ore zone are mainly iron, copper, and magnesium sulphates, whereas the lakeshore assemblage is dominated by magnesium-, calcium-, sodium-, and aluminum-bearing sulphate minerals. Near the lakeshore, the highly soluble iron sulphate salts dissolve in the lake water, increasing its iron content. Other less soluble salts are more stable and persist in the lakeshore environment. The precipitation and dissolution of efflorescent salts, and, to a lesser extent, the oxidative weathering of the remaining ore minerals, produce additional AMD. Due to the perpetual cycle of mineral dissolution and precipitation, the lake has a low pH (≈ 3) and contains high concentrations of some contaminants. The processes that contribute to the formation of the efflorescent mineral assemblages and their environmental impact on pit lake waters, and indeed the complete geochemical system, is a typical example of secondary mineral formation in Cyprus-type Cu-pyrite massive sulphide ore deposits.

Keywords Efflorescent minerals · Acid mine drainage · Pyrite oxidation · Cu-pyrite massive sulphide deposits

Introduction and Scope

The oxidative weathering of pyrite and other sulphides commonly results in the formation of sulphate minerals, the mobilization of metals, and the increase of acidity in surface and groundwater environments (Bigham and Nordstrom 2000). The sulphate minerals (efflorescent salts), which are generally formed as products of hydrolysis and evaporation, may incorporate into their crystal structure a variety of metals (Dold 2014; Hammarstrom et al. 2005; Jambor et al. 2000). The stability of the efflorescent sulphate minerals depends on temperature, relative humidity, and their composition, while reactions involving these minerals can exert a strong influence on the environment (Ranville et al. 2004; Sánchez-España et al. 2005; Valente and Leal Gomes 2009). Their formation, which reflects the interaction of the surrounding rock with surface water and groundwater, has a noticeable impact on water quality

---

Electronic supplementary material The online version of this article (doi:10.1007/s10230-016-0398-0) contains supplementary material, which is available to authorized users.

✉ Danae N. Antivachis
antivachis@gmail.com

[1] Department of Economic Geology and Geochemistry, Faculty of Geology and Geoenvironment, School of Science, National and Kapodistrian University of Athens, Panepistimiopoli, Zographou, Athens, Greece

[2] Laboratory of Mineralogy, Petrology and Economic Geology, Department of Geological Sciences, School of Mining and Metallurgical Engineering, National Technical University of Athens, Athens, Greece

[3] School of Mineral Resources Engineering, Technical University of Crete, Chania, Greece

(Gray 1997; Lu 2004; Sánchez-España et al. 2005). Because of the high solubility of many of the efflorescent sulphate minerals, climate controls mineral formation and metal mobilization; the minerals reprecipitate during dry periods (Keith et al. 2001).

In Cyprus, most of the abandoned open pit mines are associated with Cu-pyrite massive sulphide deposits. Acid mine drainage (AMD) has been generated at most of the mines and highly acidic pit lakes have formed. Studies of the mineralogy of efflorescent blooms in these mines are very limited. The secondary minerals that have been identified in pyrite ores are mostly hydrated iron-, magnesium-, and aluminum sulphates (e.g. Iron Mountain: Alpers et al. 1994; Nordstrom 1999; Nordstrom and Alpers 1999b; Iberian Pyrite Belt: Sánchez-España et al. 2005). Hudson-Edwards and Edwards (2005) studied the presence and potential remobilization of arsenic, copper, lead, and zinc in secondary minerals that formed after supergene alteration of mine waste in mine spoil heaps at the Mathiati abandoned mine (Fig. 1a). Preliminary mineralogical data

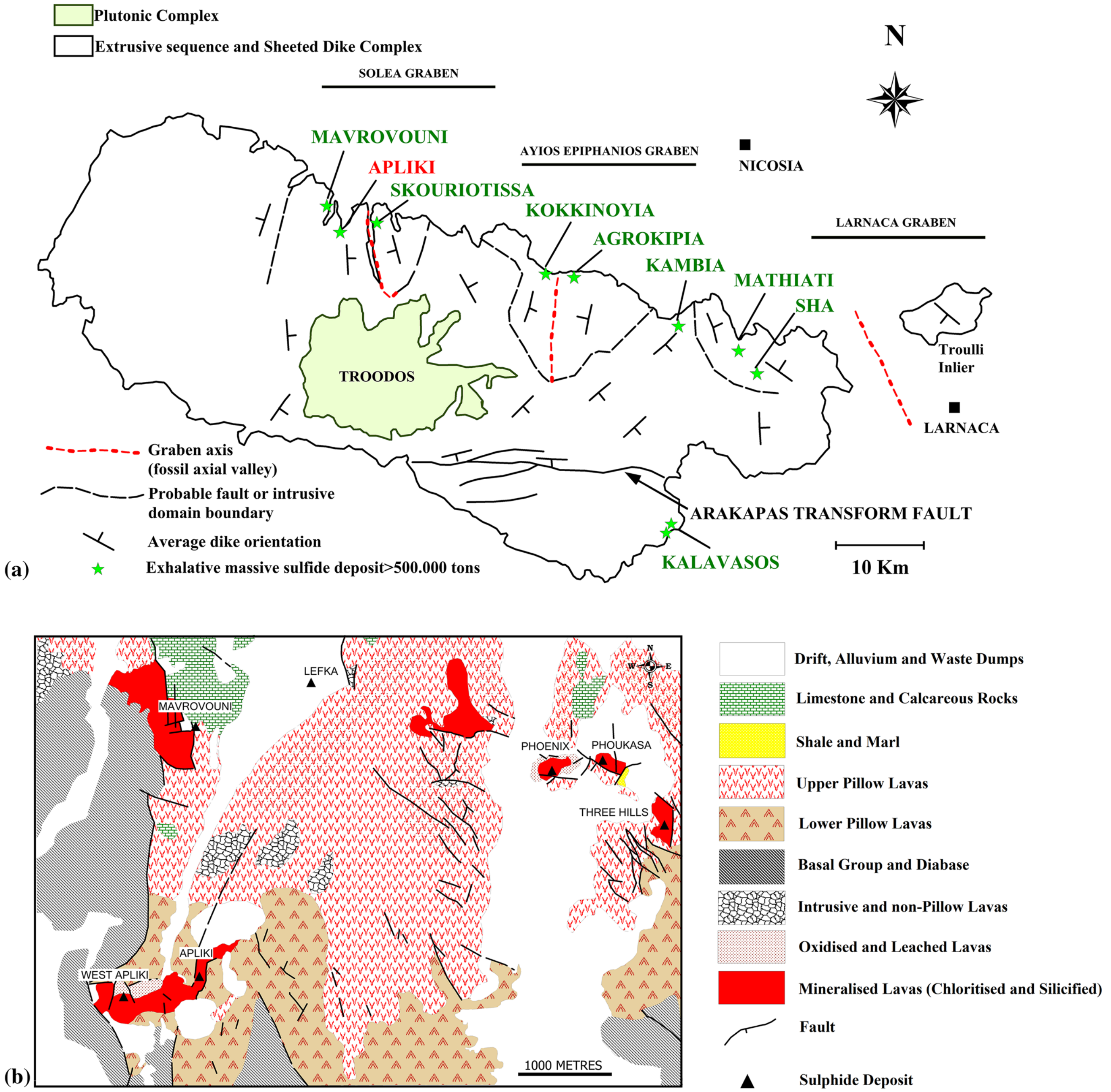

Fig. 1 **a** Generalized geological map of Cyprus showing location of the main exhalative massive sulphide deposits. The relative extent of the plutonic and the sheeted dike complex and extrusive sequence, as well as the average orientation of diabase dikes, are indicated (Varga and Moores 1985). **b** Geological map of the Skouriotissa–Mavrovouni region (Adamides 2010)

for efflorescent minerals at the Mathiati ore zone indicated that iron and magnesium sulphate salts predominated, followed by aluminum and calcium sulphate salts (Galanopoulos 2012).

According to Bigham and Nordstrom (2000), most pit lakes are acidic, with pH ranging from 2 to 4. The contamination of natural waters, due to sulphate dissolution, and the subsequent mobilization of metals may lead to severe water quality deterioration. The Apliki mine at Skouriotissa region (Figs. 1b, 2) and the existing pit lake therefore provide an ideal case study for the examination of hypogene and supergene mineral assemblages, their geochemistry, and their environmental implications during AMD generation. We studied the mineralogy of the efflorescent salts in the Cyprus-type ore deposit of Apliki to identify and understand the processes involved in their formation and assess their environmental impact.

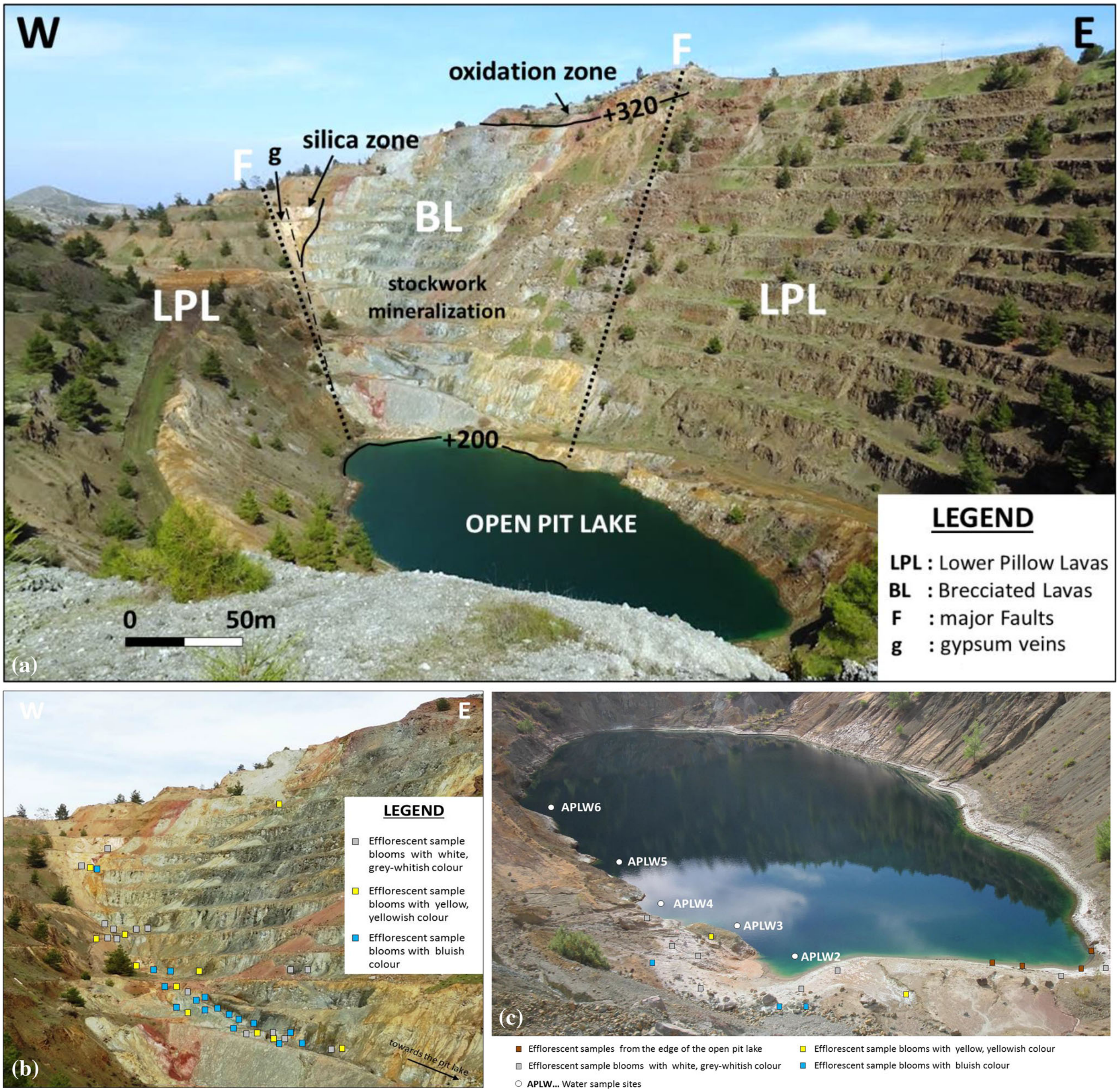

Fig. 2 **a** General view of the northern part of the Apliki abandoned mine. **b** The mineralized zone with efflorescent sample sites and field occurrences of colorful efflorescent blooms. **c** The lakeshore with efflorescent and water sample sites

Site Description

Geology of the Apliki Deposit

Cyprus' massive sulphide Cu-pyrite ore deposits have been exploited and processed, mainly for copper production, since the Bronze Age. The Apliki deposit is a typical example of a Cyprus-type ore deposit. The abandonment of the Apliki mine in the mid-1970s left a deep pit, now hosting an acidic lake fed by precipitation and surface runoff, which is surrounded by the mineralized zone and adjacent basaltic pillow lavas.

The geochemistry of pit lake waters is a critical factor for the mineralogy of hydrated sulphates at the lakeshore and provides a "guide" for minerals that can be expected to form in pit lakes elsewhere. The Apliki pit lake is at an altitude of about 200 m, and the ellipsoidal lake is 180 m long and 90 m wide. The area around the mine site is poorly vegetated, with the exception of some pine trees (Fig. 2a). The lack of detailed hydrogeological data for the mine area prevents any conclusion of a possible connection between the lake and aquifers.

The sulphide mineralization is hosted within pillow basalt (Figs. 1, 2a). The mineralogy, chemistry, and hydrothermal alteration patterns indicate that they are part of the sequence of "Lower Pillow Lavas" of the Troodos ophiolite complex (Adamides 1984). Plagioclase, pyroxenes (augite), magnetite and ilmenite, and rarely olivine are the main magmatic mineral components (Antivachis 2014). Prevailing secondary minerals, such as celadonite, calcite, analcime, and quartz occur within amygdules or are dispersed within the rock matrix, indicating that the lower pillow basalts are characterized by low-temperature regional scale alteration (Antivachis 2014).

The sulphide mineralization is tectonically controlled, developed within a hydrothermal explosion breccia zone, bounded by two steeply inclined N–S trending faults (Fig. 2a). The basaltic breccia is pervasively hydrothermally altered. Chlorite, clay minerals (smectites, kaolinite-smectites, mixed smectites, chlorite-smectites), albite, quartz, and sulphides characterize the hydrothermal alteration as chloritic. In the upper parts of the mineralized zone, weak silicification is recorded.

At Apliki, both the cupriferous massive sulphide ore and the high-grade parts of the stockwork zone have been removed by previous mining (N. Adamides, personal communication, June 18, 2015). As the massive sulphide zone has been mined out, the bulk of the examined mineralization comprises the associated stockwork zone. The remaining part of the Apliki deposit constitutes a typical example of structurally controlled stockwork-type sulphide mineralization in chlorite-bearing and silicified lavas with an overlying oxidation zone. The stockwork zone constitutes a complex network of quartz and jasper, which crosscuts the brecciated pillow lavas and are probably the outcome of explosive hydrothermal activity within the fault zone (Lydon and Galley 1986).

Semi-massive to disseminated sulphide ore is characterized by sulphur and copper content, ranging between 0.1–16 and 0.01–3.50 %, respectively. Pyrite, marcasite, and chalcopyrite are the predominant ore minerals, whereas bornite, sphalerite, galena, and barite are accessories. Goethite, hematite, chalcocite, covellite, and iron, copper, lead, aluminum, and calcium sulphates were formed in the supergene environment. Veins of gypsum, mainly parallel to the western fault, and vein-like amorphous silica bodies occur close to the western border of the mineralized zone (Fig. 2a).

Depending on the relative abundance of various minerals, efflorescent blooms appear as white, grey-whitish, green, bluish, and yellowish mineral assemblages. In the mineralized zone, efflorescent salts appear on the walls of the open pit, directly on the exposed ore mineral surfaces, on wetted surfaces on the slopes of the pit, along fractures, and around small water ponds on the mine benches. Efflorescent salts also appear at the lakeshore as coatings on rock fragments, or as a thin cover on fine-grained detrital sediment along the periphery of the lake as a result of evaporation.

Hydrological and Climatic Status of the Apliki Area

The Apliki mine constitutes a physicochemical environment that is controlled by its topography and climate. Pyrite and chalcopyrite provide an inexhaustible source of acidity and metals, leading to the generation of iron-rich solutions. The Apliki topography defines the terrain aspect and slope, which facilitates the concentration of acidic waters (supplemental Fig. 1a), its subsequent evaporation, and results in the formation of mineral phases (supplemental Fig. 1c to 1f).

The formation and distribution of efflorescent salts is inseparably related to the hydrological and climatic conditions prevailing in the study area. The hydrological characteristics of the Apliki area are typical of semi-arid Mediterranean-type climate regions. According to the data provided by the Cyprus Meteorological Service, the annual average precipitation at Apliki for the hydrological years 2010, 2011, and 2012 was just 34, 33, and 27 mm respectively. The precipitation, during sampling periods, ranged from 40–150 mm/month during winter (November–March), from 0 to 10 mm/month during spring and summer (April–October). During 2010 and 2011, the rainy period started after the sampling had taken place. Because rainwater would tend to dissolve the accumulated salts, it is deduced that the sampled efflorescent salts formed during the preceding dry period.

Materials and Methods

Sampling of efflorescent salts was performed in two periods, November 2010 and October 2011. Stainless steel spatulas were used to carefully separate the efflorescent salts from the substrate. Relative humidity and ambient temperatures in the mine during sampling ranged from 45 to 78 % and 27 to 39 °C respectively. Mineral samples were preserved into clean, dark, closed polypropylene bags, kept from sunlight and high temperatures, and immediately transported and stored in a freezer (4 °C). All samples were analyzed almost immediately to prevent mineralogical changes.

Sampling was done based primarily on the spatial distribution and color of efflorescent salts. Thus, 32 representative samples were collected, both from the mineralized zone and the lakeshore, covering an area of 10,100 m^2. In the mineralized zone, a plethora of colorful sulphate phases was observed on exposed rock surfaces, whereas at the lakeshore, the efflorescent salts were present as relatively thick, whitish to yellowish encrustations forming a rim around the lake.

The mineralogical identification and the chemical composition of the efflorescent salts were performed by combining three techniques: x-ray diffraction (XRD), RAMAN spectroscopy for mineralogical identification (in addition to optical microscopy), and scanning electron microscopy (SEM) for chemical analysis. For XRD, a Siemens D-5005 diffractometer was used. All samples were scanned between 3 and 65° 2θ angle with a velocity of 1°/min, using the Ka radiation of a Cu x-ray tube, operated with a voltage of 40 kV and a current of 40 mA. X-ray diffractograms were evaluated with EVA software, version 2.0. Chemical analyses and back-scattered imaging of samples were performed using a SEM JEOL JSM-5600 and an EDS Oxford Link Isis 300 at the Laboratory of Economic Geology and Geochemistry, National and Kapodistrian University of Athens, Greece. The microRaman instrument used in this study mainly assisted in identifying minor mineral phases in the samples, which were not easily detected by bulk XRD analyses. The instrument used is a confocal Renishaw RM1000 model, located at the National Technical University of Athens, School of Mining and Metallurgical Engineering. The spectrometer is attached to a Leica DMLM optical microscope, capable of variable magnifications up to 1000. The installed laser is a HeNe type laser, emitting at 628.8 nm, which at the highest magnification can be focused at a spot about 1.5 μm in size with energy of about 4 mJ. Most of the samples were analyzed intact, as they were sampled, often at lower magnifications and higher beam energies. The Raman spectra are collected through a 50 μm slit and analyzed with a grating type spectrometer of 1800 lines/mm. They were collected with a Peltier-cooled CCD camera in scanning mode. The acquired spectra are from 180 cm^{-1}, after the cutoff of the edge filter of the instrument, and up to 4000 cm^{-1}, to include the water peaks. Several peaks were integrated per spectrum, and were then corrected for background by fitting a set of very broad Gaussian-shaped peaks with the use of customized software.

Additionally, water samples were collected from the surface of the open pit lake in November 2010 and October 2011, following the international standards for sampling (US Environmental Protection Agency 2011). A total of ten samples of lake water (five samples per sampling period) were collected from the upper parts of the epilimnion, from a maximum depth of 2 m. Duplicate samples were collected at all sampling locations. Analyses of all samples showed a deviation of <2 %.

The location and distribution of water sampling sites are depicted in Fig. 2c. It was impossible to take water samples from greater depths in the lake. Apart from technical reasons, the acidic open pit lake is situated on the border of the Republic of Cyprus, south of the Green Line, which is controlled by UN Forces; thus, it was impossible to obtain the required permits.

Water samples were filtered in situ through a 0.45 μm pore-size Whatman membrane to remove suspended particles, stored in polyethylene bottles after acidification to pH 2 (with 1N HCl) to avoid metal precipitation, and then placed in a refrigerator at about 4–5 °C to suspend biological and chemical reactions.

Physicochemical parameters such as pH, Eh, and temperature were measured in situ with the electronic multiparameter CyberScan PCD 650, while chemical analyses were performed by ALS laboratories, Ireland, using ICP-MS. SO_4^{2-} was qualitatively estimated by ion chromatography in the Hellenic Copper Mines Ltd chemical lab. The quantitative analyses presented here were performed with a Hach DR4000 spectrophotometer of the National and Kapodistrian University of Athens, Laboratory of Economic Geology and Geochemistry, using methods 8051 and 8113 of the user's manual.

Results

Mineralogy of the Efflorescent Salts

Several hydrated iron sulphate minerals were identified in samples from the Apliki mine. The degree of iron oxidation depends on temperature, pH, Eh, relative humidity, presence of indigenous sulphur and iron-oxidizing bacteria, and

Table 1 Efflorescent minerals abundance in Apliki mine

Mineral	Nominal chemical formula[a]	Mineralized zone	Lakeshore
Mg sulphates		VH	VH
Epsomite	$MgSO_4 \cdot 7H_2O$	+	+
Hexahydrite	$MgSO_4 \cdot 6H_2O$	+	+
Pentahydrite	$MgSO_4 \cdot 5H_2O$	+	+
Starkeyite	$MgSO_4 \cdot 4H_2O$	+	+
Mg–Al sulphate		H	VL
Pickeringite	$MgAl_2(SO4)_4 \cdot 22H_2O$	+	+
Cu sulphates		H	A
Chalcanthite	$CuSO_4 \cdot 5H_2O$	+	
Langite	$Cu_9SO_4(OH)_6\ 2H_2O$	+	
Antlerite	$Cu_3SO_4(OH)_4$	+	
Fe sulphates		I	VL
Melanterite	$FeSO_4 \cdot 7H_2O$	+	
Copiapite	$Fe_{14}O_3(SO_4)_{18}(OH) \cdot 63H_2O$	+	
Halotrichite	$FeAl_2(SO_4)_4 \cdot 22H_2O$	+	
Siderotil	$(Fe,Cu)SO_4 \cdot 5H_2O$	+	+
Fibroferrite	$FeSO_4(OH) \cdot 5H_2O$	+	+
Jarosite	$KFe_3{}^{3+}(OH)_6(SO_4)_2$		+
Bilinite	$Fe^{2+}Fe^{3+}(SO_4) \cdot 22H_2O$		+
Ca sulphate		I	H
Gypsum	$CaSO_4 \cdot 2(H_2O)$	+	+
Na sulphate		L	L
Thenardite	Na_2SO_4	+	+
Na–Mg sulphates		L	H
Bloedite	$Na_2Mg(SO_4)_2 \cdot 4H_2O$	+	+
Conyaite	$Na_2Mg(SO_4)_2 \cdot 5H_2O$	+	+
Loeweite	$Na_{12}Mg_7(SO_4)_{13} \cdot 15H_2O$	+	
Na–Ca sulphates		VL	A
Glauberite	$Na_2Ca(SO_4)_2$	+	
Watevillite	$Na_2Ca(SO_4)_4\ 22H_2O$	+	
Al sulphates		L	VL
Alunogen	$Al_2(SO_4)_3 \cdot 17(H_2O)$	+	+

Abundance: *VH* very high, *H* high, *I* intermediate, *L* low, *VL* very low, *A* absent, *M* mineralized zone, *L* lakeshore

[a] Nominal chemical formulas from Martin et al. (1999), Mandarino (1999), Jerz and Rimstidt (2003) and Hammarstrom et al. (2005)

the exposure of mineral surfaces to these conditions. The identity and frequency of occurrence of various efflorescent minerals in both sampling areas at Apliki are listed in Table 1. Pyrite and chalcopyrite are relict sulphides in some of the samples. Example spectra of single-phase efflorescent minerals identified by microRaman are provided in Fig. 3, while their peak identification is discussed in supplemental Appendix I and summarized in supplemental Table 1 of the file. Most of the samples collected from the Apliki mine are characterized by an assemblage of mineral phases, whereas single phases are rarely observed. Hydrous magnesium sulphates-mainly epsomite ($MgSO_4 \cdot 7H_2O$), either as a single mineral or mixed with other secondary minerals-are the predominant mineral constituents of the efflorescence, both in the mineralized zone and at the lakeshore, followed by gypsum. Iron and copper sulphates develop exclusively in close proximity to the dense stockwork of Cu-pyrite mineralization and rarely along the lakeshore.

Most iron sulphates occur in places protected from atmospheric precipitation and out of contact with water, which explains their limited existence on the lakeshore and more frequent occurrence in samples with limited exposure in the mineralized zone (Table 1). The mineralogical composition of efflorescent salts in the mineralized zone indicated that melanterite (Fe^{2+}), copiapite (Fe^{2+}/Fe^{3+}), and halotrichite

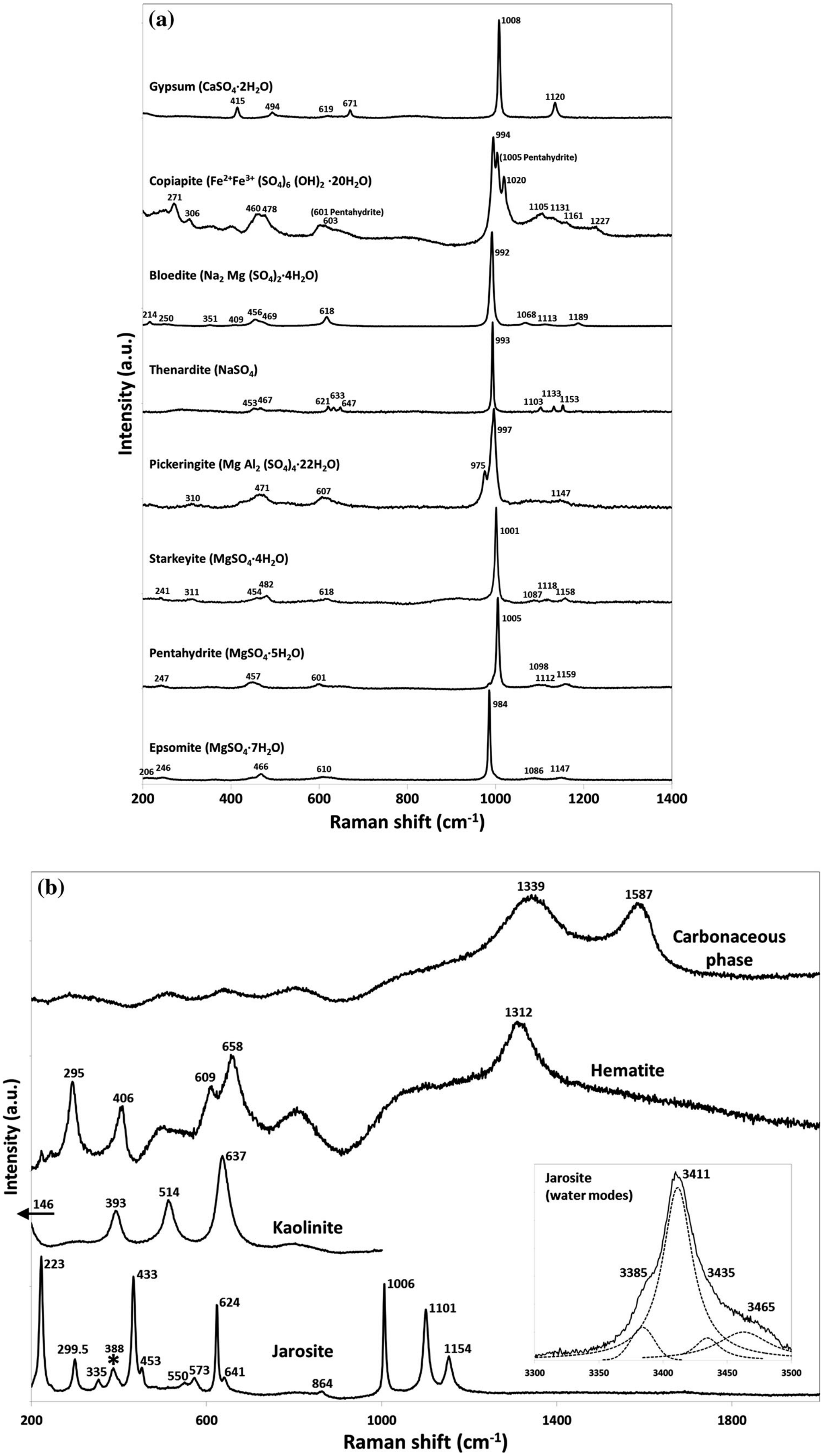

Fig. 3 **a** Raman spectra of major efflorescent minerals identified in the Apliki mine. **b** Raman spectra of jarosite, kaolinite, hematite, and a carbonaceous phase identified intermixed with the efflorescent minerals in the samples from the Apliki mine

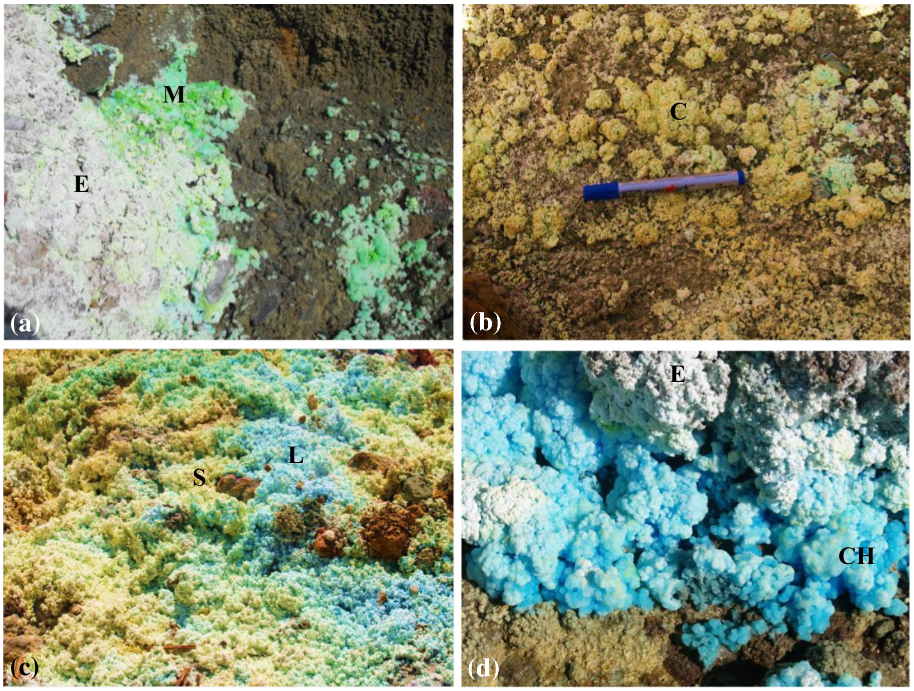

Fig. 4 Field occurrences of efflorescent sulphate minerals precipitating from acid mine drainage on weathered surface of mineralized zone: **a** melanterite (*M*) and epsomite (*E*); **b** copiapite (*C*) probably forming from oxidation of melanterite; **c** efflorescent blooms with langite (*L*) and siderotil (*S*) and; **d** general aspect of the efflorescence, including chalcanthite (*CH*) and epsomite (*E*)

(Fe^{2+}/Fe^{3+}) predominated (Fig. 4), while siderotil (Fe^{2+}) and fibroferrite (Fe^{3+}) were less abundant. On some mine benches, near dense stockwork, melanterite appeared as a thick encrustation (Fig. 4a) and sometimes was gradually oxidized to copiapite (Fig. 4b). The iron minerals at the lakeshore were very limited in abundance and spatial distribution. The dominant iron minerals were siderotil (Fe^{2+}) and fully oxidized (Fe^{3+}) jarosite; bilinite (Fe^{2+}/Fe^{3+}) and fibroferrite (Fe^{3+}) may also have been present. These minerals are formed by evaporation and coexist with gypsum, magnesium–aluminum sulphate (pickeringite) and sodium-magnesium sulphate (bloedite), forming thin white coatings (Table 1; Supplemental Fig. 1d).

In the mineralized zone, three copper sulphates, chalcanthite, langite, and antlerite, were identified (Table 1; Fig. 4 and supplemental fig. 2). Chalcanthite was the predominant mineral, followed by langite, and rarely antlerite. These minerals are limited in spatial distribution, restricted by the dense stockwork of Cu-pyrite mineralization.

Magnesium sulphates were present in both the mineralized zone and at the lakeshore (Fig. 2c; Table 1). The capacity of the magnesium minerals to withstand dissolution contributes to their continued spatial distribution towards the lake.

In the mineralized zone, a variety of calcium, sodium, and magnesium sulphates were identified, from the completely anhydrous member (i.e. thenardite), to other hydrated members, whose abundance in the mineralized zone was very limited compared with the corresponding ones at the lakeshore (Table 1), forming efflorescent blooms as thick accumulations covering the exposed rock surfaces (Fig. 4 and supplemental fig. 1). Small crystallites of gypsum ($CaSO_4{\cdot}2H_2O$), under the microscope and with microRaman, demonstrate very characteristic spectra (for details, see supplemental file Appendix I). Additionally, pickeringite and alunogen (aluminum sulphates) were identified in small abundance at the lakeshore (Table 1, supplemental Fig. 3).

Geochemistry of Pit-Lake Water

The Apliki lake water was acidic (pH $\approx$ 3), with an Eh of $\approx + 202$ mV, demonstrating weakly oxidizing conditions. In the first sampling period (Nov. 2010), water pH was 2.7, while in the second (Oct. 2011), pH had increased to 3.2. The Eh and SO_4^{2-} concentrations remained approximately the same (Table 2). Water temperature increased in the second sampling period by 7 °C, from 17.7 to 24.7 °C (Table 2). These deviations in pH and temperature reflect the intense and prolonged drought in 2010 and the diluting rainfall that followed. This drought contributed to the extensive formation of efflorescent blooms, which subsequently dissolved with the first rains in 2011 and enriched the Apliki lake water in dissolved constituents. The physicochemical characteristics of the lake water reflect the homogeneity of the upper parts of epilimnion, since no significant change was observed from one sampling point to another during a particular sampling event.

The lake water had elevated concentrations of SO_4^{2-} (16,103 mg/L), copper (323 mg/L), iron (18 mg/L), and

Table 2 Physicochemical characteristics of Apliki pit lake waters, based on samples collected in November 2010 (2010) and October 2011 (2011)

Sample	pH		T (°C)		Eh (mV)		SO_4^{2-} (mg/L)	
	2010	2011	2010	2011	2010	2011	2010	2011
APLW2	2.7	3.2	17.9	24.8	205	198	15,390	15,950
APLW3	2.8	3.3	18.2	24.5	205	198	16,710	16,310
APLW4	2.7	3.1	18.1	24.7	206	197	16,200	16,310
APLW5	2.6	3.1	17.3	24.5	209	199	16,620	16,020
APLW6	2.7	3.1	17.4	24.6	206	197	16,040	15,480
Mean	2.7	3.2	17.7	24.7	206	197.8	16,192	16,014
Minimum	2.6	3.1	17.3	24.5	205	197	15,390	15,480
Maximum	2.8	3.3	18.2	24.8	209	199	16,710	16,310

zinc (59 mg/L) from oxidative dissolution of pyrite, chalcopyrite, and, to a lesser extent, other sulphide minerals present in the deposit, such as sphalerite (for details, see Table 3). Additionally, concentrations of calcium (529 mg/L), sodium (2032 mg/L), magnesium (2164 mg/L), potassium (12.3 mg/L), and aluminum (162 mg/L) were high due to weathering of the pillow lavas (for details, see Table 3). The average concentrations of the potentially toxic elements, namely copper, zinc, cobalt, and nickel, were slightly higher in 2011 (Table 3). The most notable change was the increased copper concentrations, from an average value of 289 mg/L in 2010 to 357 mg/L in 2011. Geochemical results from earlier studies (Charalambides et al. 1998) indicate that the Apliki lake waters have the highest copper concentrations compared with other open pit lakes in Cyprus.

Discussion

Mineral Efflorescence Formation Processes: Genesis in the Mineralized Zone

At Apliki, it is evident that sulphide mineral oxidation has resulted in the formation of a variety of secondary minerals, which play an important role in trace metal cycling between aqueous and solid solutions. The oxidation of pyrite and marcasite led to the formation of melanterite, a mineral that forms in Fe^{2+} rich water, according to the following reaction (Hammarstrom et al. 2005, and references therein):

$$Fe^{2+}_{(aq)} + SO^{2-}_{4(aq)} + 7\,H_2O \underset{\text{(melanterite)}}{\longrightarrow} FeSO_4 \cdot 7\,H_2O_{(s)} \tag{1}$$

Melanterite is a precursor mineral for other iron sulphate minerals (Bigham and Nordstrom 2000; Hammarstrom et al. 2005; Jambor et al. 2000; Komnitsas et al. 1995; Triantafyllidis and Skarpelis 2006; Triantafyllidis et al. 2007). The temperature and humidity of the Apliki mine favors melanterite stability, compared to less hydrous phases. However, dehydration of melanterite occurs with parallel substitution of iron with copper, Both melanterite and siderotil occur in close proximity to the dense stockwork of Cu-pyrite mineralization. This proximity, along with topography and rainfall, then control the precipitation-dissolution cycle and subsequent mineral transformations (Figs. 2b, 4).

According to Sánchez-España et al. (2008), once the acidic Fe^{2+}–Fe^{3+}–H^+–$SO_4{}^{2-}$ rich solutions accumulate in small ponds on the mine benches, water is partly evaporated and melanterite precipitates when the Fe^{2+} and $SO_4{}^{2-}$ concentrations exceed the solubility product for this mineral (Marion et al. 2008). The conversion of melanterite to siderotil reflects decreasing moisture, complemented by increasing temperatures or lower humidity, and incorporation of copper (Jambor et al. 2000). Gradually, ferrous iron (Fe^{2+}) is oxidized to ferric iron (Fe^{3+}), and melanterite is converted to copiapite during wet periods. In Apliki, however, it seems that melanterite is oxidized to copiapite after it is exposed to the atmosphere under acidic conditions. The reaction that takes place during this process is the following (Buckby et al. 2003):

$$\begin{aligned} &Fe^{2+} + 3Fe^{3+} + 6SO_4^{2-} + 22H_2O \underset{\text{(copiapite)}}{\longrightarrow} \\ &Fe_4(SO_4)_6(OH)_2 20H_2O + 2H^+ \end{aligned} \tag{2}$$

Jerz and Rimstidt (2003) state that copiapite is stable in an environment where humidity is around 65 %, while it begins to dissolve when humidity levels exceed 80 %, generating very acidic leachates (Nordstrom and Alpers 1999a).

The Fe^{3+} minerals ferricopiapite and fibroferrite, which were also found in the mineralized zone, represent an even more advanced stage in the oxidation sequence, with gradual transition of early divalent iron salts of melanterite and siderotil to mixed divalent and trivalent iron salts of copiapite and halotrichite, in accordance to the literature (e.g. Jerz 2002; Nordstrom 1999;). Halotrichite was also present in the mineral assemblage of Apliki, and is

Table 3 Chemical composition of Apliki pit lake waters, based on samples collected in November 2010 (2010) and October 2011 (2011)

Sample	Cu (mg/L)		Fe (mg/L)		Zn (mg/L)		Mg (mg/L)		Ni (mg/L)		Ca (mg/L)	
	2010	2011	2010	2011	2010	2011	2010	2011	2010	2011	2010	2011
APLW2	262	351	17	17	50	64	1990	2100	1.7	2.3	477	528
APLW3	289	368	19	15	53	68	2150	2210	1.8	2.4	519	555
APLW4	301	360	20	17	54	66	2250	2160	1.9	2.1	536	539
APLW5	297	354	21	18	54	66	2250	2180	1.8	2.2	530	543
APLW6	294	354	20	20	54	65	2230	2120	1.8	2.0	529	534
Mean	289	357	19	17	53	66	2174	2154	1.8	2.2	518	540
Minimum	262	351	17	15	50	64	1990	2100	1.7	2.0	477	528
Maximum	301	368	21	20	54	68	2250	2210	1.9	2.4	536	555
Average value	323		18		59		2164		2.0		529	
Detection limit	0.04		2		0.04		2		0.02		2	

Sample	Cd (mg/L)		Co (mg/L)		Al (mg/L)		Mn (mg/L)		Na (mg/L)		K (mg/L)	
	2010	2011	2010	2011	2010	2011	2010	2011	2010	2011	2010	2011
APLW2	0.6	0.8	4.1	5.2	139	164	150	168	1816	1994	11	12
APLW3	0.7	b.d	4.4	5.4	154	174	162	176	2001	2122	13	12
APLW4	0.7	b.d	4.5	5.4	157	169	168	172	2106	2049	13	12
APLW5	0.7	0.8	4.6	5.5	162	172	169	173	2105	2044	13	12
APLW6	0.7	0.7	4.5	5.3	161	166	167	170	2054	2032	13	12
Mean	0.7	0.8	4.4	5.4	155	169	163	172	2016	2048	13	12
Minimum	0.6	<0.7	4.1	5.2	139	164	150	168	1816	1994	11	12
Maximum	0.7	0.8	4.6	5.5	162	174	169	176	2106	2122	13	12
Average value	0.75		4.9		162		168		2032		12.3	
Detection limit	0.02	0.7	0.02		2		0.1		0.1		2	

b.d below detection limit

probably formed according to the following reaction (Hammarstrom et al. 2005, and references therein):

$$Fe^{2+}_{(aq)} + 4\,SO^{2-}_{4(aq)} + 2\,Al^{3+}_{(aq)} + 22\,H_2O \rightarrow FeAl_2(SO_4)_4{\cdot}22H_2O \qquad (3)$$

The presence of halotrichite indicates late stages of a paragenetic sequence of copiapite, through dehydration, after the formation of iron sulphates, which is reflected by its spatial distribution. Particularly, halotrichite rarely coexists with iron sulphates (i.e. copiapite) and it only forms efflorescent blooms with magnesium, magnesium–aluminum, and copper sulphates. According to Chou and Seal (2003, 2007), the formation of magnesium sulphate minerals, and the transition from one to another as a function of changing humidity, is controlled by the following general reaction:

$$MgSO_4 \cdot nH_2O \leftrightarrow MgSO_4 \cdot m\,H_2O + (n{-}m)\,H_2O, \quad n > m \qquad (4)$$

The dominance of epsomite, hexahydrite, pentahydrate, and starkeyite associations is probably due to the abundant supply of Mg from the basalt. Under acidic conditions, the dissolution of chlorite is probably the main Mg source, while clinopyroxenes (augite) from the adjacent basaltic pillows may be an additional source.

At Apliki, epsomite is the most abundant sulphate mineral because it is the most stable mineral over a wide temperature range and its solubility decreases in acidic conditions (Al-Jibbouri et al. 2002). Chou and Seal (2003) have defined the phase equilibria between epsomite-hexahydrite as a function of temperature and humidity. Any changes to these factors lead either to hydration or dehydration reactions ($n = 6$ hexahydrite, $n = 5$ pentahydrite, $n = 4$ starkeyite, $n = 2$ santerite, $n = 1$ kieserite). Stable phase equilibria for the system $MgSO_4$-H_2O as a function of temperature and relative humidity as well as more pertinent details, are presented in Appendix II and summarized in supplemental Fig. 4. There are assemblages of epsomite-hexahydrite, hexahydrite-pentahydrite-starkeyite, or hexahydrite-pentahydrite in the mineralized zone, demonstrating their rather unstable nature.

The most abundant calcium-sodium-magnesium minerals were gypsum and thenardite, while bloedite and konyaite were less frequently observed. Loeweite, glauberite, and watevilleite were also most probably present.

Gypsum is stable in almost all weather conditions in Cyprus over a broad temperature range (Appendix II; supplemental Fig. 5; Hammarstrom et al. 2005; Spencer 2000). Gypsum, unlike the previous minerals, is not an acid-forming mineral phase, and does not contribute to acidity generation or neutralization.

The weathering of aluminosilicates in the host rock results in the formation of a variety of soluble aluminum sulphates, including pickeringite and alunogen. Pickeringite is the magnesium end-member of the halotrichite-pickeringite solid solution (Cody and Grammer 1979; Martin et al. 1999). According to Blowes et al. (2004), the formation of soluble salts containing aluminum (halotrichite-pickeringite series and alunogen) is paragenetically later than that of magnesium salts (epsomite, hexahydrite etc.) and calcium sulphate (gypsum). This delay is because the main sources of aluminum are the aluminosilicate minerals of the surrounding volcanic rocks, the dissolution of which is typically slow and requires low-pH conditions to accelerate the process.

Chalcanthite is stable in environments where pH ranges from 2.0 to 6.5 (supplemental Fig. 6a; Yoder et al. 2007) and in a wide range of temperatures and relative humidity (supplemental Fig. 6b; Chou et al. 2002), in contrast to langite, which is formed at a relatively higher pH, from 5.6 to 7.1 (Alwan and Williams 1979). It is noted that in acidic environments created by pyrite oxidation, chalcanthite is the only stable phase (Chou et al. 2002), which advocates and supports its dominant presence in the mineralized zone relative to antlerite.

Mineral Efflorescence Formation Processes: Genesis on the Lakeshore

Oxidation of sulphides in the mineralized zone and secondary mineral formation on the pit walls results in neoformation of efflorescence at the lakeshore. As oxidation progresses, drainage water on the slope of the open pit becomes more acidic. Iron is fully oxidized and saturation of solutions leads to the precipitation of less soluble minerals, such as jarosite, together with iron oxides and hydroxides. The acidity of waters increases according to the following reactions (Bigham and Nordstrom 2000):

$$Fe^{3+} + 2H_2O \rightarrow FeOOH + 3\,H^{+} \tag{5}$$

$$K^{+} + 3\,Fe^{3+} + 2\,SO_4^{2-} + 6\,H_2\mathrm{O} \rightarrow KFe_3^{3+}(SO_4)_2(OH)_6 + 6\,H^{+} \tag{6}$$

In the lakeshore, jarosite is found only along the edge of the lake, due to the high acidity (Table 2), and coexists with gypsum. Its presence is however limited (small crystals identified only with microRaman; Fig. 3b). The mineral formation sequence at the lakeshore is similar to that in the mineralized zone. The mineral formation reactions have been reported by Bandy (1938), Jambor et al. (2000), Nordstrom and Alpers (1999a), and Velasco et al. (2005).

The predominant calcium-sodium-magnesium minerals (Table 1) are gypsum, bloedite, konyaite, epsomite, whereas hexahydrite, pentahydrite, starkeyite and thenardite are less abundant. These efflorescent mineral assemblages are common in acidic environments (Freyer and Voigt 2003; Hill 1937; Leduc et al. 2009; Spencer 2000), where they occur as thick coatings, and have the ability to transform from one to another. Such a transformation is demonstrated at the Apliki mine by the co-existence of these minerals (Fig. 2b, c).

The dominance of calcium-sodium-magnesium sulphates (e.g. epsomite, bloedite, thenardite) at the lakeshore over the iron and copper sulphates (e.g. copiapite, chalcanthite) is due to the instability of the latter, as their hydration state changes under atmospheric conditions.

Dissolution of copper sulphates explains copper enrichment in the pit lake waters (i.e. values of 323 mg/L) (Table 3). The higher copper concentration between the two sampling periods (from 289 to 357 mg/L) is possibly due to differences in chemistry of the drainage water from the slopes of the mineralized zone.

The dominant aluminum sulphates at the lakeshore are pickeringite and alunogen. It should be mentioned that an increase in humidity or any other change in the microenvironment where these minerals are formed, i.e., a pH change, triggers the dissolution process. Therefore, at the lakeshore, either the increased humidity, or the precipitation, or both led to the dissolution of aluminum sulphate phases, contributing to their limited presence at the lakeshore (Table 1).

Conclusions

The mineral efflorescence in the Apliki mine occurs as complex mineral assemblages. The abundance, variety, and chemical composition of sulphate minerals are inherently linked with the chemical composition of the ore and the low neutralization capacity of the host pillow lavas. A clear dominance of magnesium, iron, and copper sulphates is observed in the mineralized zone, while at the lakeshore of the pit lake, magnesium-calcium-sodium-aluminum sulphates are more abundant.

The exposure of fresh surfaces of sulphide minerals (mainly pyrite and chalcopyrite) to atmospheric fallout contributes to acid generation, and consequently metal ion mobility. The sulphate anions are then fixed in secondary sulphate minerals through evaporation or neutralization reactions that lead to supersaturation of the water with respect to secondary minerals (Lottermoser 2010). The formation of efflorescent salts in the mineralized zone plays a crucial role in the transient accumulation of acidity and metals (Jambor et al. 2000). The soluble salts, such as iron and copper sulphates, in the proximity of the dense stockwork zone, as well as of other salts along the mine benches, sequester and subsequently release trace metals. Their dissolution, during wet periods, or by surface water flows, leads to the generation of additional acidity, promoting the superficial acid drainage and the existence of ponds, thus regulating the chemical composition of the water and the existing oxidation conditions. The AMD is characterized by high concentrations of SO_4^{2-} and metals, indicating the oxidation and the subsequent dissolution of pyrite and accompanying sulphides (chalcopyrite, marcasite, and sphalerite). These acidic solutions can infiltrate the primary minerals, increase their acidity, and ultimately enter the lake, enriching the water with metals. The Apliki open pit lake can be considered a typical lake for an abandoned Cyprus-type open pit mine, characterized by high concentrations of metals and acidity.

The Apliki ore deposit provides the opportunity for a holistic study of the system “country rock-ore-efflorescent salts-lake waters”. Ore oxidation triggers a sequence of complex oxidation-dehydration-neutralization reactions, which leads to the subsequent formation of magnesium, iron, and copper efflorescent salts. The AMD downgrades the quality of the lake water, decreases pH, and increases the concentrations of toxic metals and sulphate. The observed mineralogical assemblages and their spatial development in the mineralized zone demonstrate that the cycle of mineral precipitation-dissolution is closely associated with ore chemistry, water availability, and its evaporation.

The sulphate minerals at Apliki exert a strong environmental influence on the lake. Ore oxidation, the subsequent formation of secondary minerals and the dehydration and dissolution reactions leads to the generation of more acidity and the extensive release of metals, which in turn affect pit lake water chemistry. The efflorescent salts at the lakeshore reflect this chemistry.

The combination of oxidation-hydration/dehydration-acidification/neutralization reactions determines the formation of the secondary minerals. Therefore, the formation sequence of the Apliki sulphate minerals and their resulting spatial distribution can be used as a reference model for other similar deposits in similar climates and topographic settings, even where, instead of a pit lake, a stream or a river is in the vicinity of an open pit.

Acknowledgments This study of the Apliki ore deposit was partially funded by the “Papadakis Scholarship Foundation” and a research grant to Prof. N. Skarpelis by the Special Account for Research Grants (Kapodistrias Program) of the University of Athens. The authors acknowledge “Hellenic Copper Mines Ltd.”, and especially its Director General, Mr. Konstantinos Xydas, for hospitality and logistical support, as well as Dr. Nicos Adamides, Senior Geologist, for his fieldwork support and for being a constant source of information and data on the Troodos Ophiolite Complex. We also thank Mr. Evangelos Michaelidis, Department of Economic Geology and Geochemistry, University of Athens, for his assistance with SEM work, and Assistant Professor Maria Perraki, National Technical University of Athens, for a very preliminary mineralogical identification of sulphate minerals by RAMAN Spectroscopy.

References

Adamides NG (1984) Cyprus volcanogenic sulphide deposits in relation to their environment of formation. Unpublished Ph.D. Thesis, University of Leicester, UK

Adamides NG (2010) Mafic-dominated volcanogenic sulphide deposits in the Troodos Ophiolite, Cyprus, part 1—the deposits of the Solea Graben. T I Min Metall B 119(2):65–77

Al-Jibbouri S, Strege C, Ulrich J (2002) Crystallization kinetics of epsomite influenced by pH-value and impurities. J Cryst Growth 236:400–406

Alpers CN, Nordstrom DK, Thompson JM (1994) Seasonal variations of Zn/Cu ratios in acid mine water from Iron Mountain, California. In: Alpers CN, Blowes, DW (eds) Environmental geochemistry of sulphide oxidation, vol 550. American Chemical Society Symposium Series, pp 324–344

Alwan AK, Williams PA (1979) Mineral formation from aqueous solution, part ii, the stability of langite, $Cu_4SO_4(OH)_6 \cdot H_2O$. Transit Metal Chem 4:319–322

Antivachis DN (2014) Ore deposit geology and environmental impacts from exploitation of the Apliki mine, Skouriotissa mining district, Cyprus. Unpublished Ph.D. Thesis, Department of Economic Geology and Geochemistry, National and Kapodistrian University of Athens, Greece

Bandy MC (1938) Mineralogy of three sulphate deposits at Northern Chile. In: Nordstrom DK (ed) The Effect of sulphate on aluminium concentrations in natural waters: Some stability relations in the system Al_2O_3–SO_3–H_2O at 298 K. Geochim Cosmochim Acta, vol 4, pp 681–692

Bigham JM, Nordstrom DK (2000) Iron and aluminum hydroxysulphates from acid sulphate waters. Rev Miner Geochem 40(1):351–403

Blowes DW, Ptacek CJ, Jambor JL, Weisener CG (2004) The geochemistry of acid mine drainage. Treatise Geochem 9:149–204

Buckby T, Black S, Coleman ML, Hodson ME (2003) Fe-sulphate-rich evaporative mineral precipitates from the Rio Tinto, Southwest Spain. Miner Mag 67(2):263–278

Charalambides A, Kyriacou E, Constantinou C, Baker J, van Os B, Gurnari G, Shiathas A, van Dijk P, van der Meer F (1998) Mining waste management on Cyprus: assessment, strategy development and implementation. EU DG-XT-LIFE project-94/CYJB2J1CYI0977IMED, final report II, hydrochemical and geochemical data, geological survey department, Nicosia

Chou I-M, Seal RR (2003) Acquisition and evaluation of thermodynamic data for morenosite–retgersite equilibria at 0.1 MPa. Am Miner 88(11–12):1943–1948

Chou I-M, Seal RR II (2007) Magnesium and calcium sulphate stabilities and the water budget of Mars. J Geophys Res 112(E11):10

Chou I-M, Seal RR, Hemingway BS (2002) Determination of melanterite-rozenite and chalcanthite-bonattite equilibria by humidity measurements at 0.1 MPa. Am Miner 87:108–114

Cody AD, Grammer TR (1979) Magnesian halotrichite from White Island. New Zealand. J. Geol. Geophys 22(4):495–498

Dold B (2014) Submarine tailings disposal (STD)—a review. Minerals 4:642–666

Freyer D, Voigt W (2003) Crystallization and phase stability of $CaSO_4$ and $CaSO_4$-based salts. Monatsh Chem 134:693–719

Galanopoulos E (2012) Weathering processes of massive sulfide Cu-FeS_2 mineralization and mining waste of the abandoned Mathiatis mine, Cyprus and environmental impacts: neutralization tests of acid mine drainage. M.Sc Thesis, Department of Economic Geology and Geochemistry, National and Kapodistrian University of Athens, Greece

Gray NF (1997) Environmental impact and remediation of acid mine drainage: a management problem. Environ Geol 30(1/2):62–71

Hammarstrom JM, Seal RR II, Meier AL, Kornfeld JM (2005) Secondary sulphate minerals associated with acid drainage in the Eastern US: recycling of metals and acidity in surficial environments. Chem Geol 215:407–431

Hill AE (1937) The transition temperature of gypsum to anhydrite. J Am Chem Soc 59:2242–2244

Hudson-Edwards KA, Edwards SJ (2005) Mineralogical controls on storage of As, Cu, Pb and Zn at the abandoned Mathiatis massive sulphide mine, Cyprus. Miner Mag 69:695–706

Jambor JL, Nordstrom DK, Alpers CN (2000) Metal-sulphate salts from sulfide mineral oxidation. Rev Miner Geochem 40(1):303–350

Jerz JK (2002) Geochemical reactions in unsaturated mine wastes. Ph.D. Thesis, Blacksburg, VA, University Libraries, Virginia Polytechnic Institute and State University, vol OCLC, p 49698307

Jerz JK, Rimstidt JD (2003) Efflorescent iron sulphate minerals: paragenesis, relative stability. Am Miner 88:1919–1932

Keith DC, Runnells DD, Esposito KJ, Chermak JA, Levy DB, Hannula SR, Watts M, Hall L (2001) Geochemical models of the impact of acidic groundwater and evaporative salts on Boulder Creek at Iron Mountain, California. Appl Geochem 16:947–961

Komnitsas K, Xenidis A, Adam K (1995) Oxidation of pyrite and arsenopyrite in sulphidic spoils in Lavrion. Miner Eng 8(12):1443–1454

Leduc EMS, Peterson RC, Wang R (2009) The crystal structure and hydrogen bonding of synthetic conyaite, $Na_2Mg(SO_4)_2 \cdot 5H_2O$. Am Mineral 94:1005–1011

Lottermoser BG (2010) Mine wastes: characterization, treatment, and environmental impacts, 3rd edn. Springer, Berlin

Lu M (2004) Pit lakes from sulphide ore mining, geochemical and limnological characterization before treatment, after liming and sewage sludge treatments. Unpublished Ph.D. Thesis, Lulea University of Technology, Department of Chemical Engineering and Geosciences

Lydon JW, Galley A (1986) Chemical and mineralogical zonation of the Mathiati alteration pipe, Cyprus and its genetic significance. In: Ixer RA, Neary CR, Prichard HM (eds) Gallagher MJ. Metallogeny of basic and ultrabasic rocks London, Inst Min Metall, pp 49–68

Mandarino JA (1999) Fleischer's glossary of mineral species. Mineralogical record, Tucson

Marion GM, Kargel JS, Catling DC (2008) Modeling ferrous-ferric iron chemistry with application to Martian surface geochemistry. Geochim Cosmochim Act 72:242–266

Martin R, Rodgers KA, Browne PRL (1999) The nature and significance of sulphate-rich aluminous efflorescences from the Te Kopia geothermal field, Taupo volcanic zone, New Zealand. Miner Mag 63:413–419

Nordstrom DK (1999) Efflorescent salts and the effects on water quality and mine plugging. Mine Water Environ IMWA Int Congress, Sevilla 2:543–546

Nordstrom DK, Alpers CN (1999a) Geochemistry of acid mine waters. In: Plumlee GS, Logsdon MJ (eds) The environmental geochemistry of mineral deposits, part A: processes, techniques and health issues. Rev Econ Geol, vol 6A, pp 133–160

Nordstrom DK, Alpers CN (1999b) Negative pH, efflorescent mineralogy, and consequences for environmental restoration at the Iron Mountain Superfund site, California. Proc Natl Acad Sci USA 96:3455–3462

Ranville M, Rough D, Flegal AR (2004) Metal attenuation at the abandoned Spenceville copper mine. Appl Geochem 19(5):803–815

Sánchez-España J, Lopez Pamo E, Santofimia Pastor E, Aduvire O, Reyes J, Beretti D (2005) Acid mine drainage in the Iberian Pyrite Belt (Odiel river watershed, Huelva, SW Spain): geochemistry, mineralogy and environmental implications. Appl Geochem 20:1320–1356

Sánchez-España J, Lopez Pamo E, Santofimia Pastor E, Diez Ercilla M (2008) The acidic mine pit lakes of the Iberian Pyrite Belt: an approach to their physical limnology and hydrogeochemistry. Appl Geochem 23:1260–1287

Spencer RJ (2000) Sulphate minerals in evaporite deposits, reviews in mineralogy and geochemistry. Miner Soc Am 40(1):173–192

Triantafyllidis S, Skarpelis N (2006) Mineral formation in an acid pit lake from a high-sulphidation ore deposit: Kirki, NE Greece. J Geochem Explor 88:68–71

Triantafyllidis S, Skarpelis N, Komnitsas K (2007) Environmental characterization and geochemistry of Kirki, Thrace, NE Greece, abandoned flotation tailing dumps. Environ Forensics 8(4):351–359

U.S. Environmental Protection Agency (2011) Drinking water standards and health advisories, EPA 820-R-11-002. Office of Water U.S. Environmental Protection Agency, Washington

Valente TM, Leal Gomes C (2009) Occurrence properties and pollution potential of environmental minerals in acid mine drainage. Sci Total Environ 407:1135–1152

Varga RJ, Moores EM (1985) Spreading structure of the Troodos ophiolite, Cyprus. Geology 13:846–850

Velasco F, Alvaro A, Suarez S, Herrero J-M, Yusta I (2005) Mapping Fe-bearing hydrates sulphate minerals with short wave infrared (SIR) Spectral analysis at San Miguel mine environment, Iberian Pyrite Belt (SW Spain). J Geochem Explor 87(2):45–72

Yoder CH, Agee TM, Ginion KE, Hofmann AE, Ewanichak JE, Schaeffer CD Jr, Carroll MJ, Schaeffer RW, McCaffrey PF (2007) The relative stabilities of the copper hydroxyl sulphates. Miner Mag 71(5):571–577